Water molecular reorientation in ice and tetrahydrofuran clathrate hydrate from lineshape analysis of 17O spin-echo NMR spectra

Ba, Yong; Ripmeester, John A.; Ratcliffe, Christopher I.

Publisher's version / Version de l'éditeur:
https://doi.org/10.1139/v11-040
Canadian Journal of Chemistry, 89, 9, pp. 1055-1064, 2011-08-19

Water molecular reorientation in ice and tetrahydrofuran clathrate hydrate from lineshape analysis of ^{17}O spin-echo NMR spectra

Yong Ba, John A. Ripmeester, and Christopher I. Ratcliffe

Abstract: Lineshape analysis of ^{17}O spin-echo NMR spectra has been used to study water molecular reorientations in ice-Ih and THF Structure II clathrate hydrate. The kinetics was determined by the changes of the lineshapes of the ^{17}O central transitions at different temperatures. A model involving 12 orientations and 4-step jumps of water molecular orientations was proposed. Semi-classical exchange formalism was employed to simulate the lineshape of the central transitions of the ^{17}O nuclei. Lineshape analysis gave the quadrupolar coupling constant $C_Q = 6.43$ MHz and the asymmetry parameter $\eta = 0.935$, for both ice-Ih and THF gas hydrate. The theoretical lineshape simulations resulted in activation energies of water molecular reorientations $E_a = 55.2 \pm 2.1$ kJ mol^{-1} and $E_a = 30.5 \pm 0.8$ kJ mol^{-1} for ice-Ih and THF hydrate, respectively. The range of dynamic rates in THF clathrate hydrate is such that before melting, a pseudo-isotropic lineshape is observed that retains a second-order quadrupolar shift. The water reorientation process is discussed in light of recent results on Bjerrum defect injection obtained from molecular dynamics simulation and structural studies.

Key words: Ice-Ih, THF clathrate hydrate, ^{17}O NMR, molecular reorientations of solid water, Kinetics, residual second order quadrupolar shift, dynamics of non-integer quadrupolar nuclei.

Résumé : On a fait appel à l'analyse de la forme des raies des spectres RMN du ^{17}O avec écho de spin pour étudier les réorientations moléculaires de l'eau dans la glace-Ih et dans l'hydrate du clathrate du THF de structure II. On a déterminé les cinétiques par les changements dans les formes des raies des transitions centrales du ^{17}O, à diverses températures. On propose un modèle impliquant 12 orientations et des transitions en quatre étapes des orientations moléculaires de l'eau. On a utilisé un formalisme d'échange semi-classique pour simuler la forme des raies des transitions centrales du noyau ^{17}O. Une analyse de la forme des raies permet de déterminer la constante de couplage quadripolaire $C_Q = 6{,}43$ Mhz et le paramètre d'asymétrie $\eta = 0\,935$ pour la glace-Ih et l'hydrate du THF gazeux. Les simulations des formes des raies théoriques ont permis d'évaluer les énergies d'activation des réorientations moléculaires de l'eau $E_a = 55{,}4 \pm 2{,}1$ kJ mol^{-1} et $E_a = 30{,}4 \pm 0{,}8$ kJ mol^{-1}, respectivement pour la glace-Ih et l'hydrate du THF. La plage des vitesses dynamiques pour l'hydrate du clathrate du THF est telle que, avant la fusion, il et possible d'observer une forme de raie pseudo-isotrope qui conserve un déplacement quadripolaire du deuxième ordre. On discute du processus de réorientation de l'eau à la lumière de résultats récents sur l'injection du défaut de Bjerrum obtenu à partir de simulations de la dynamique moléculaire et d'études structurales.

Mots-clés : glace-Ih, hydrate du clathrate du THF, RMN du ^{17}O, réorientations moléculaires de l'eau solide, cinétique, déplacement quadripolaire résiduel du second ordre, dynamique des noyaux quadripolaires non entiers.

[Traduit par la Rédaction]

Introduction

Water, as a substance essential for the existence of life, is one of the most important materials in nature. Also, it is one of the more difficult materials to study as it has some unusual properties and a remarkably complex phase diagram.

When frozen under normal atmospheric conditions, water molecules form a crystalline solid with hexagonal symmetry that is less dense than the water phase with which it is in equilibrium, referred to as hexagonal ice or ice-Ih.[1] Early X-ray diffraction analysis of ice-Ih showed that each oxygen atom is coordinated almost tetrahedrally by four neighboring oxygen atoms.[2] From neutron diffraction measurements on a

Received 16 November 2010. Accepted 3 February 2011. Published at www.nrcresearchpress.com/cjc on XX XXXX) 2011.

Y. Ba. Steacie Institute for Molecular Sciences, National Research Council of Canada, 100 Sussex Drive, Ottawa, ON, K1A 0R6, Canada; Department of Chemistry and Biochemistry, California State University Los Angeles, 5151 State University Drive, Los Angeles, California 90032, USA.

J.A. Ripmeester and C.I. Ratcliffe. Steacie Institute for Molecular Sciences, National Research Council of Canada, 100 Sussex Drive, Ottawa, ON, K1A 0R6, Canada.

Corresponding author: Christopher I. Ratcliffe (e-mail: chris.ratcliffe@nrc-cnrc.gc.ca).

This paper is dedicated to professor Rod Wasylishen to honour his many outstanding contributions in the field of NMR spectroscopy and to chemistry in Canada.

single crystal of D_2O solid, it was suggested that there are two half-occupied deuteron positions on the line between two neighboring oxygen atoms,[3] and the deuterons are disordered among these sites. This conclusion was later modified from the view that the O–D–O hydrogen bond should be bent by about 6.8°, since the molecular D–O–D angle is the same as that in an isolated water molecule (i.e., 104.5°).[4] Thus, each deuteron is about 0.04 Å off the line connecting the two closest oxygen atoms. These experimental data fit into Pauling's earlier statistical model for the structure of ice-Ih.[5] He proposed that (*i*) the structure of isolated water molecules is primarily preserved in ice-Ih, (*ii*) the hydrogen atoms of a water molecule are directed approximately towards two of the four oxygen atoms surrounding it tetrahedrally, (*iii*) The adjacent water molecules are oriented so that only one hydrogen atom lies between each pair of neighboring oxygen atoms, and (*iv*) the statistical orientations of water molecules generate a large number of configurations $(3/2)^n$, where n is the total number of water molecules. At any instant and under ordinary conditions, an ice-Ih crystal may exist in any one of the large number of allowed configurations. A question that follows then is whether the configuration of ice-Ih is subject to change via rotations of water molecules. Dielectric relaxation studies have suggested that the dipole moment of ice can reorient through either proton transfer or molecular rotation.[6,7] The latter was assumed based on theoretical considerations to correlate the rotational correlation time with the dielectric correlation time.[8] Bjerrum hypothesized that water molecules in ice could reorient by rotating about one hydrogen bond and form either a D defect (two hydrogen atoms between a pair of oxygen atoms) or an L defect (no hydrogen atom between a pair of oxygen atoms).[9] When these defects diffuse through the lattice, they leave a water molecule in a different orientation.

Clathrate hydrates are formed when water interacts hydrophobically with suitably small molecules (<0.9 nm), assembling via hydrogen bonding into an open framework that traps such "guest" molecules into cages of different geometries.[10–15] Three main structural types of clathrate hydrate have been identified, which form with a large number of guests, namely cubic structure I, cubic structure II, and hexagonal structure H.[10–20] Tetrahydrofuran (THF) forms a structure II hydrate popular for experimental studies as it can be made readily by freezing an aqueous solution of the correct composition.[19] The unit cell contains 136 water molecules with 16 small and 8 large cages. The large cages each encage a THF molecule. A neutron diffraction study of $3.5Xe{\cdot}8CCl_4{\cdot}136D_2O$ structure II gas hydrate shows that the local coordination of a water molecule is very similar to that in ice-Ih, although deviation from true tetrahedral coordination by four neighbouring O atoms is more marked.[20] Indeed there are three crystallographically distinct O sites. Also, as in ice-Ih, the D_2O molecules are disordered over six orientations of equal statistical weight, with deuterium atoms located in half-occupied sites, so a gas hydrate crystal also has many configurations determined by the orientations of all the water molecules.

Solid state NMR lineshapes are widely used to study dynamics.[21] Changes in the linewidth and lineshape as a function of increasing temperature reflect the effects of rapid modulation of the interaction tensors, and there are very many examples involving dipolar coupling tensors, for example of ^1H, ^{19}F, integer quadrupolar tensors, especially ^2H,[22,23], and chemical shift tensors, ^{13}C, ^{15}N, ^{19}F, etc. However, reports of cases involving dynamic averaging of the lineshapes of non-integer nuclei with second-order quadrupolar interactions are quite rare.

The reorientations of water molecules in ice-Ih and THF clathrate hydrate as a function of temperature have been observed previously for ^1H [24–30] and ^2H NMR.[28,31–36] Approaching their melting points, the spectra show isotropic lineshapes. In ^2H NMR, the results can be explained by a simple model where each O–D bond jumps between four equiprobable tetrahedral orientations, although in this model the gross approximation is made that the ^2H quadrupolar coupling tensor is axial. Unfortunately the models that can explain the experimental observables do not necessarily test the theoretical models, such as the Bjerrum model. For instance, a water molecule would have to be visited by several defects in order for it to be reoriented in such a way as to show tetrahedral averaging. Nevertheless the ^1H, ^2H and dielectric results can be explained by the presence of a single motional correlation time. One striking feature of THF clathrate hydrate is that the motions are considerably faster than in ice, and it is thought that this is due to injection of Bjerrum L-defects into the hydrate lattice by transient H-bond formation between the O atom of the THF and a water molecule.[37]

Here we present work on the central transition NMR of the spin 5/2 ^{17}O nucleus in ice and THF structure II clathrate hydrate as a function of temperature. In contrast with the four orientations visited by the ^2H quadrupole coupling tensor, the tensor of ^{17}O in the water molecule will reorient over six orientations as the arrangement of H atoms around it changes (in this case roughly octahedral orientations), and so in a sense the ^{17}O detects the motion of the whole molecule rather than of the O–D bond. Another reason for a study using ^{17}O is because the proton-shielding tensor in ice-Ih has a span of ~6 kHz, the ^1H dipolar coupling leads to spectra ~40 kHz wide, the deuterium quadrupolar coupling constant is ~200 kHz, and the ^{17}O quadrupolar coupling constant is ~6.43 MHz. Although the ^{17}O central transitions in ice are expected to cover a spectral width of ~60 kHz, complete averaging of the quadrupolar interaction can give spectral sensitivity to a remarkably broad range of motional correlation times. Besides the problem of water molecular reorientations, there is a wide interest in the fundamental spectroscopy, that is, to observe and understand the evolution of spectral patterns for half-integer nuclei from a static pattern to one where the quadrupolar coupling is completely averaged.[38–43]

Because of the ubiquitous presence of water in its various phases, we expect considerable relevance of these results to water-containing systems.

Experimental details

Water with 45% ^{17}O (ISOTEC Inc.) and THF with 99.9% purity (Sigma-Aldrich) were used to prepare the ice and hydrate. THF is soluble in water, so that the clathrate hydrate was easily obtained by cooling its aqueous solution with 1:17 THF/H_2O stoichiometric ratio.[44] ^{17}O NMR static spectra with ^1H decoupling were obtained at 40.68 MHz from 140 K

Fig. 1. Static ^{17}O NMR ^{1}H decoupled spin-echo spectra of the central transition in ice-Ih as a function of temperature.

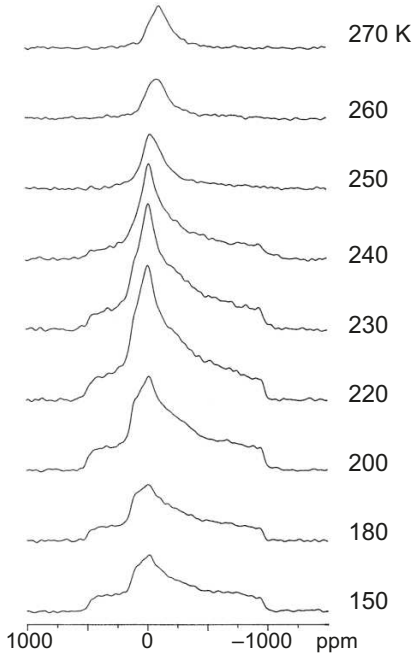

up to the melting points, using a Bruker AMX 300 NMR spectrometer with a double resonance (^{1}H-^{17}O) high-power NMR probe (Morris Instruments Inc.). Only central transition spectra were obtained, using a spin-echo experiment with $\tau = 20$ μs.[45] ^{1}H decoupling is necessary, as the ^{17}O-^{1}H dipolar coupling is calculated to be of the order of 17 kHz, compared with ~59 kHz for the ^{17}O second-order static linewidth. The spectra are referenced to liquid $H_2{}^{17}O$ water at room temperature. Temperatures were regulated using cold nitrogen gas and a Bruker Eurotherm controller.

Results and discussion

The ^{17}O NMR central transition spectra of ice-Ih and THF clathrate hydrate as a function of temperature are shown in Figs. 1 and 2. The lowest temperature spectra correspond to essentially static quadrupolar coupling tensors. For ice-Ih at 150 K, the best theoretically fitted spectrum gave a quadrupolar coupling constant $C_Q = 6.43$ MHz and an asymmetry parameter $\eta = 0.935$. This compares favourably with previous measurements, which have given $C_Q = 6.66 \pm 0.10$ and $\eta = 0.935 \pm 0.010$ for D_2O ice-Ih at 253–263 K,[46] and $C_Q = 6.525 \pm 0.015$ and $\eta = 0.925 \pm 0.020$ at 77 K.[47] The first of these studies also determined that the principal axis components of the tensor are oriented with *yy* perpendicular to the molecular plane and *xx* along the twofold molecular axis. C_Q is moderately sensitive to the local environment of the water molecules, as seen in the different values for water-^{17}O in Ice-II ($C_Q = 6.893$ MHz, $\eta = 0.865$),[48] and crystal hydrates oxalic acid dihydrate ($C_Q = 6.8$ MHz, $\eta = 0.93$)[49] and barium chlorate monohydrate ($C_Q = 7.61$ MHz, $\eta = 0.94$).[50] For THF clathrate hydrate at 140 K, the envelope of the spectrum is somewhat noisier than that of ice-Ih, perhaps because of an inhomogeneous orientational distribution of hydrate crystallites produced when the THF solution was frozen in the NMR probe. Nevertheless, it is clear that the lineshape is almost identical to that of ice-Ih at 150 K, and thus we conclude that the local oxygen coordination in THF clathrate hydrate is very similar to that in ice-Ih. Though there are three crystallographically distinct water oxygen sites in the THF hydrate,[19,20] these are not distinguished in the static lineshapes observed, nor even in the dynamically averaged pseudo-isotropic lineshapes observed at the highest temperatures.

Fig. 2. Static ^{17}O NMR ^{1}H decoupled spin-echo spectra of the central transition in THF clathrate ^{17}O-hydrate as a function of temperature.

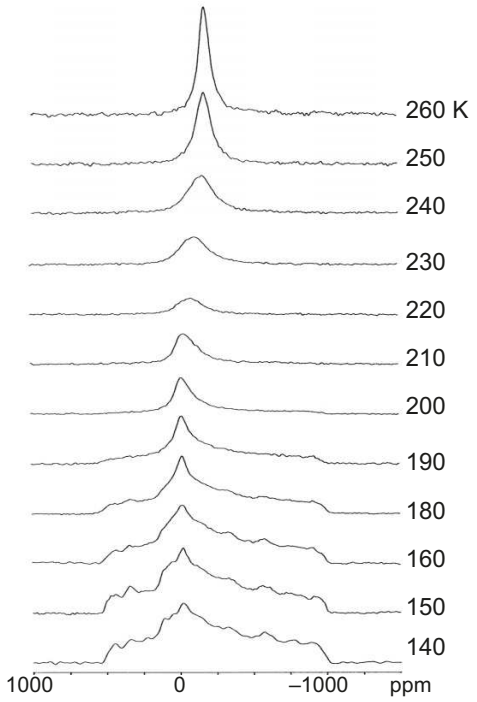

One question to consider is whether the chemical shielding anisotropy (csa) of ^{17}O in ice is large enough to make a visible contribution to the central transition spectrum at 7.05 T. While there is no experimental information available on this, ab initio calculations for liquid water suggest a span of ~37 ppm.[51] This is very small (~2.5%) when compared to the observed static linewidth of ~1450 ppm but substantial enough to perhaps explain the range of experimental values. Spectra at high field would probably resolve this issue, e.g., at 21.1 T the second-order linewidth would reduce to about 161 ppm. Furthermore, at rates where the second-order quadrupolar lineshape begins to show effects of dynamic averaging, this csa will likely already be averaged to zero.

As temperature increases, the lineshapes start to show effects of dynamic averaging; their features become less well-defined, and a new shape centred around the center of gravity of the line begins to form. Comparing the spectra of the two materials, it is immediately obvious that the dynamics in the THF hydrate are considerably faster than in ice-Ih, with equivalent changes in lineshape occurring about 50 degrees lower for THF hydrate. Initially the new lineshape is asymmetric, with its peak closest to the strongest feature of the static lineshape, but then it gradually shifts to lower frequency, and in the case of THF hydrate eventually takes on a pseudo-isotropic appearance (ice-Ih melts before this stage

Fig. 3. Static ^{17}O NMR ^{1}H decoupled spectrum of water-^{17}O in a THF clathrate hydrate sample at ~270 K, where partial melting has occurred.

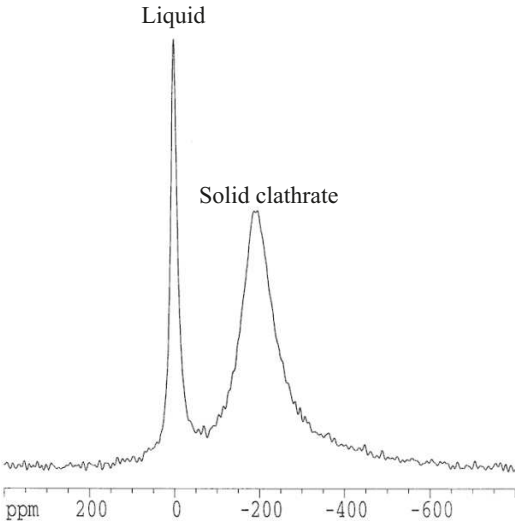

can be reached). That this "isotropic" line still retains a second-order shift is illustrated by the spectrum of the hydrate at 270 K, where liquid THF solution and solid THF hydrate coexist (Fig. 3). The liquid line is considerably sharper and very close to the shift of water, whereas the broader "isotropic" line of the hydrate is centred at –194 ± 3 ppm. The second-order quadrupolar shift of the central transition for a non-integer quadrupolar nucleus is given by,

$$[1] \quad \text{SOQS (in ppm)} = -\left(\frac{10^5}{3}\right)\left(\frac{\omega_Q^2}{\omega_L^2}\right)\left(I(I+1)-\frac{3}{4}\right)\left(1+\frac{\eta^2}{3}\right)$$

where $\omega_Q = 6\pi C_Q/(2I(2I–1))$. Hence, for a spin I = 5/2 nucleus this becomes SOQS = $–6\,000(C_Q^2/\nu_L^2)(1+\eta^2/3)$. Substituting the C_Q and η determined from the low-temperature static lineshape, a second-order shift of –193.6 ppm is calculated, very close to that observed at the melting point.

The emergence of this pseudo-isotropic line was initially quite surprising, because the central transition lineshape depends on the second-order interaction, which is a function of the fourth-order Legendre polynomial, and therefore averaging due to rapid tetrahedral or octahedral reorientation at rates a little faster than the static central transition linewidth should *not* lead to a pseudo-isotropic lineshape (icosahedral averaging is required to achieve an isotropic line).[40] In fact, the dynamic averaging calculations described below also suggest that there should be a residual lineshape, and the initial experimental averaged shapes appear to be falling into the predicted pattern. However, the modeling does not take into account the fact that at higher rates of motion the satellite transitions will also begin to average, and for I = 5/2 the splitting of the first satellite transition $\nu_Q = 3C_Q/20$, which in this case is only 964.5 kHz.

Witschas and Eckert have studied a case for ^{23}Na NMR approaching the fast motion limit, where the first-order interaction is averaged to zero, and observed a pseudo-isotropic central transition line, which gradually shifts to the true isotropic position as the satellites also average to isotropic.[41] In the present study, although the THF hydrate residual second-order lineshape has averaged to pseudo-isotropic, the material melts before any shifting towards the true isotropic shift has begun.

Fig. 4. The 12 possible orientations of a water molecule on any one particular lattice site in ice-Ih and clathrate hydrates, if the two H atoms are distinguished. O–H chemical bonds are represented by bold bars, and O···H hydrogen bonds from neighbouring water molecules by thin lines. The arrows indicate the four single-step reorientations which can occur by rotation about each of the two O–H chemical bonds for any one particular starting orientation. Over time, all 12 orientations will be sampled.

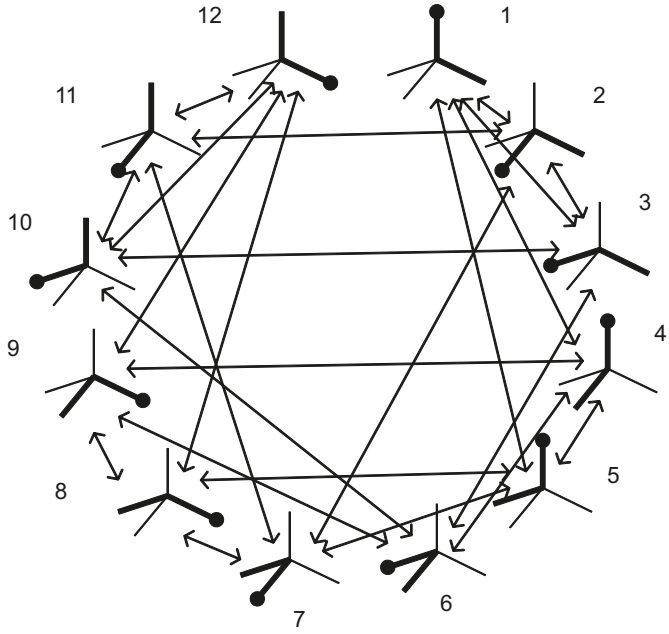

Modelling the effects of dynamic exchange on the central transition lineshape

An examination of the possible orientations for a single water molecule in ice-Ih or a clathrate hydrate shows that if the protons are distinguished, there are 12 different orientations of equal probability (Fig. 4). Assuming a single-step jump about an O-H axis only (not about O–H hydrogen bond axes) is required for the reorientational change, then each of the 12 orientations can have 4 possible single-step jumps to the other orientations. With the simplifying approximation that the coordination is perfectly tetrahedral, then all of these single-step reorientations are equivalent in terms of their kinetic parameters, as are forward and reverse exchanges. In fact this is a very reasonable assumption based on the structure of ice-Ih, but a little less so for the THF clathrate hydrate with three crystallographically distinct O atoms and some angles with larger deviations from Td. While this model provides a more complete picture of water reorientation (compared with the 4-site tetrahedral jump model used to simulate the dynamic deuterium NMR spectra of D_2O ice-Ih),[28] as far as the ^{17}O tensor is concerned, pairs of orientations related by interchange of the two proton positions are equivalent. The population of these molecular orientations in an ice or a clathrate hydrate powder determines the

Table 1. Euler angles of water molecular reorientations in ice-Ih.

Orientations	α	β	γ
1	0	0	0
2	215.2644	60	35.2644
3	144.7356	60	324.7356
4	35.2644	60	215.2644
5	324.7356	60	144.7356
6	90	90	90
7	270	90	270
8	324.7356	120	35.2644
9	35.2644	120	324.7356
10	144.7356	120	215.2644
11	215.2644	120	144.7356
12	0	180	180

Fig. 5*a*. Calculated spin-echo NMR spectra of ^{17}O central transitions for the model of 12 reorientations and 4-step jumps of water molecules in ice-Ih with $\chi = 6.43$ MHz and the hypothetical values for $\eta = 0.9$. The exchange rate constants and spin-echo amplitudes (EA) are given along with the corresponding spectra. The intensity unit is arbitrary.

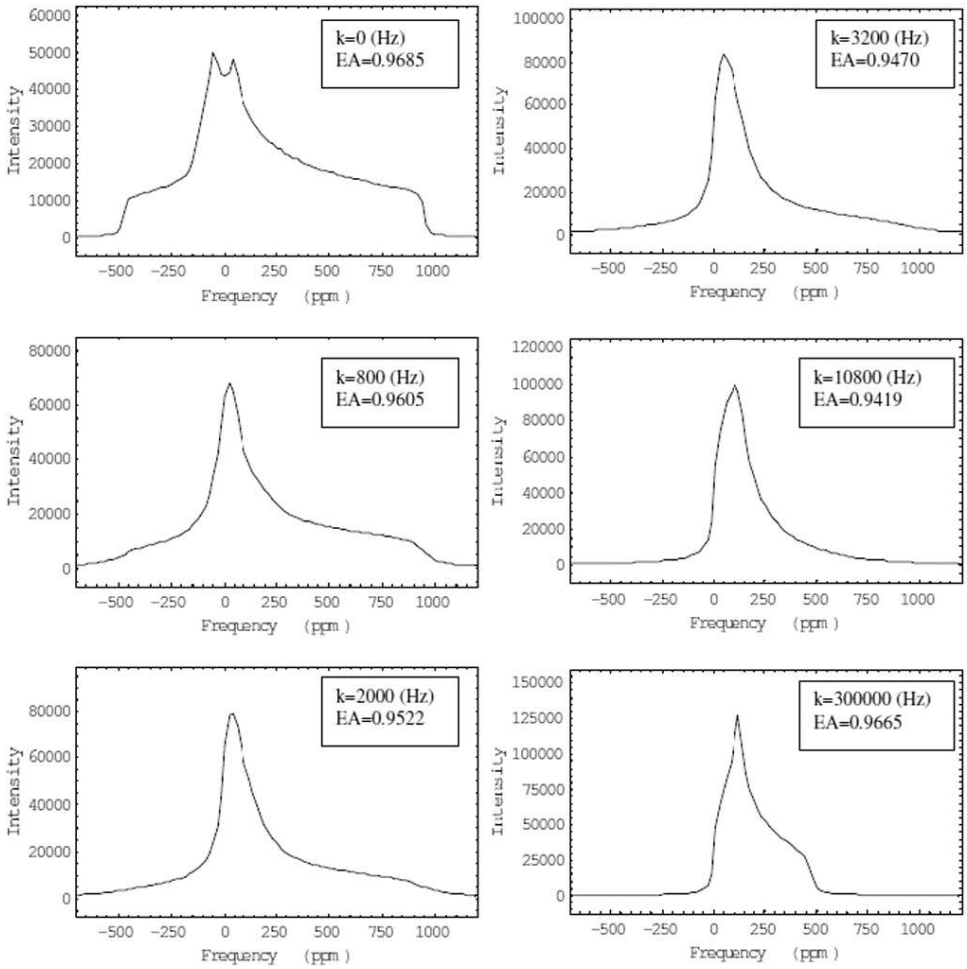

lineshape of the NMR spectrum within the slow regime of the reorientational exchange at low temperatures, and the rate constants of the reorientations determine the lineshapes at higher temperatures.

A semi-classical exchange formalism was employed to simulate the lineshapes of the ^{17}O central transitions.[40] The relevant Hamiltonian for the exchanging quadrupolar nucleus consists of the first-order chemical shift term, and the first- and second-order quadrupolar interaction terms. Owing to the time scale of the molecular reorientations observed in the ice and the clathrate hydrate, it was assumed that the exchange rates are localized in the second-order quadrupolar term, while the effect on the lineshape by the first order quadrupolar interaction is insignificant. The calculations were further simplified by ignoring the effect of chemical shift anisotropy, which as discussed earlier is likely to be negligibly small com-

Fig. 5*b*. Calculated spin-echo NMR spectra of ^{17}O central transitions for the model of 12 reorientations and 4-step jumps of water molecules in ice-Ih with $\chi = 6.43$ MHz and the hypothetical values for $\eta = 0.5$. The exchange rate constants and spin-echo amplitudes (EA) are given along with the corresponding spectra. The intensity unit is arbitrary.

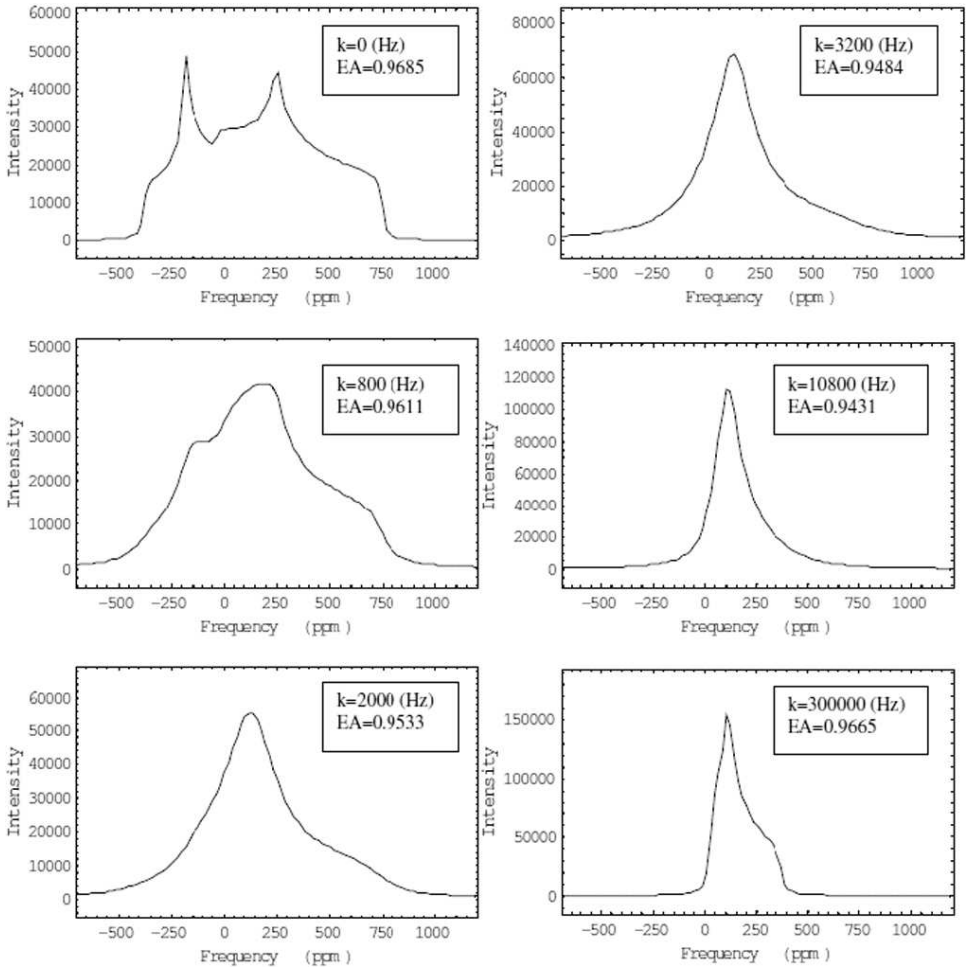

pared with the linewidth caused by the quadrupolar second-order interaction at this field, and also averaged to zero by the dynamics at quite slow rates. The relevant evolution frequency for the central transition is given as follows,[52]

$$[2] \qquad \omega^{(2)static}_{-1/2,\,1/2} = -\frac{1}{6\omega_0}\left[\frac{3C_Q}{2I(2I-1)}\right]^2\left[I(I+1)-\frac{3}{4}\right] \times [A(\alpha,\ \eta)\cos^4\beta + B(\alpha,\eta)\cos^2\beta + C(\alpha,\eta)]$$

where

$$A(\alpha,\eta) = -\frac{27}{8} + \frac{9}{4}\eta\cos 2\alpha - \frac{3}{8}(\eta\cos 2\alpha)^2$$

$$B(\alpha,\eta) = \frac{30}{8} - \frac{1}{2}\eta^2 - 2\eta\cos 2\alpha + \frac{3}{4}(\eta\cos 2\alpha)^2$$

$$C(\alpha,\eta) = -\frac{3}{8} + \frac{1}{3}\eta^2 - \frac{1}{4}\eta\cos 2\alpha - \frac{3}{8}(\eta\cos 2\alpha)^2$$

and C_Q stands for the quadrupolar coupling constant. The Euler angles α and β define the direction of the static magnetic field relative to the principal axis system of the electric field gradient.

The principal axis system of the electric field-gradient tensor of ^{17}O in the water molecule has been determined previously.[46] The *x*-axis was assigned to have the direction of the C_2 axis, the *y*-axis is perpendicular to the H–O–H plane, and the *z*-axis lies in the plane parallel to the H–H line. The twelve sets of Euler angles for water molecular orientations, as shown in Fig. 4, were derived according to this principal axis system and are listed in Table 1.

A Mathematica computer program was written to solve the equations of the kinetically modified Bloch equations,[40] and to integrate over the polar and azimuthal angles to get the powder pattern of the NMR spectrum. Figures 5*a*–5*c* show three sets of calculated ^{17}O spectra according to the exchange model shown in Fig. 4, based on a quadrupolar coupling constant of 6.43 MHz and asymmetry parameters,$\eta = 0.9$, 0.5, and 0.1, respectively. The corresponding exchange rate constants are given along with the spectra, and the spin-echo amplitudes (EA) are also shown in the figures. The transverse relaxation time $T_2 = 2.5$ ms and a spin-echo time of $\tau = 20$ us were used in the calculations. The steps for the increments for α and β were set to be 1°, and a total of 100 points along the chemical shift axis were calculated. The chemical shifts were obtained according to the ^{17}O resonance frequency of 40.68 MHz (300 MHz for ^1H). The chemical shifts in the spectra were labeled with the opposite signs because of the convenient use of the Mathematica plotting method. The

Fig. 5*c*. Calculated spin-echo NMR spectra of ^{17}O central transitions for the model of 12 reorientations and 4-step jumps of water molecules in ice-Ih with $\chi = 6.43$ MHz and the hypothetical values for $\eta = 0.1$. The exchange rate constants and spin-echo amplitudes (EA) are given along with the corresponding spectra. The intensity unit is arbitrary.

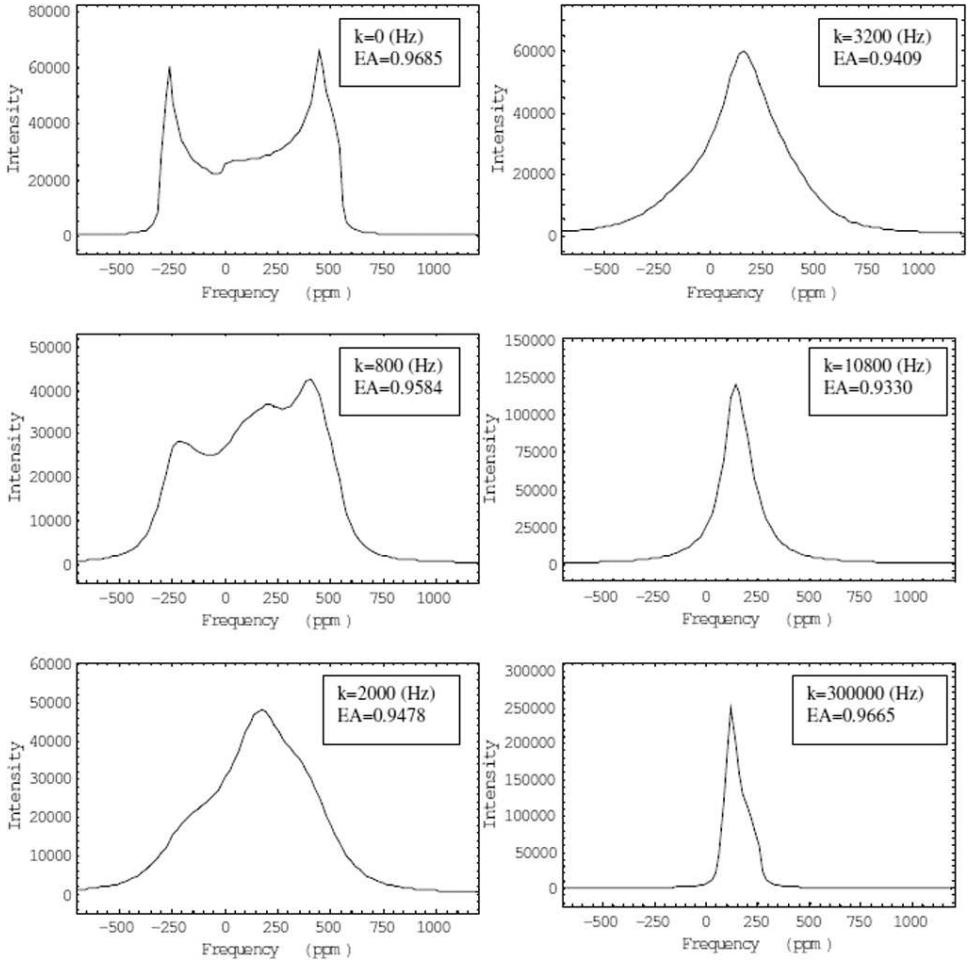

spectra at the rate constant $k = 0$ Hz show the typical powder patterns of the central transitions for spin n/2 nuclei with the corresponding hypothetical asymmetry parameters. The spectra at $k = 300\ 000$ Hz show the powder patterns in the fast-exchange regimes. Powder patterns corresponding to for other intermediate exchange rates are also shown. All three sets show residual anisotropic lineshapes in the regime where rates are fast compared with the static second-order linewidth, but again it should be emphasized that these calculations do not take account of effects when the satellite lineshapes are also being averaged.

Comparison of experimental and simulated lineshapes in the exchange regime

Experimental ^{17}O spin-echo spectra acquired at several temperatures and the corresponding theoretically simulated spectra with $C_Q = 6.43$ MHz and $\eta = 0.935$ are shown in Fig. 6. Above the temperatures shown, the experimental and simulated spectra begin to diverge and comparison is no longer valid. Activation energies were determined from the set of rate constants and temperatures using the Arrhenius law,

$$[3] \qquad k = A \exp\left(-\frac{E_a}{RT}\right)$$

where A is a frequency factor (s^{-1}), E_a is the activation energy (J mol^{-1}), and R is the gas constant (8.314 JK^{-1} mol^{-1}).

Plots of $\ln(k)$ versus $1/T$ are shown in Fig. 7. The least-squares linear fit for the ice-Ih data gave an activation energy $E_a = 55.2 \pm 2.1$ kJ?mol^{-1}. This value, within error, is the same as the value of 56.5 kJ mol^{-1}, determined from the dielectric relaxation study,[6,7] showing that the activation energy measured in the dielectric relaxation arose from the water molecular reorientations. It is also equivalent to the most recent value of $E_a = 55.6$ kJ mol^{-1}, determined from ^2H NMR lineshapes.[26] Earlier studies gave values in the range 55.2 to 59.8 kJ mol^{-1}.[24–27,31] It is interesting that although the model used in the study of D_2O ice-Ih only considered the reorientations of O–D chemical bonds in a tetrahedral fashion, the activation energy is the same as that obtained in the current work for which the more rigorous model of 12 orientations and 4 single-step jumps was used. This is probably because of the nearly axially symmetric deuterium quadrupolar coupling tensor, which in principle results in nearly similar calculated ^2H NMR lineshapes when either model is used.

The least-squares linear fit for THF clathrate hydrate resulted in an activation energy $E_a = 30.5 \pm 0.8$ kJ mol^{-1}, which is comparable to values of 31.0 kJ mol^{-1} from dielectric,[37] 30.12 kJ mol^{-1} from ^1H NMR,[30] and 31.0–32.7

Fig. 6. Experimental ^{17}O ^{1}H decoupled spin-echo NMR spectra at several temperatures shown on the left and matching dynamic simulation spectra shown on the right, for (*a*) ice-Ih and (*b*) THF clathrate hydrate. The temperatures and rate constants are given alongside the corresponding spectra.

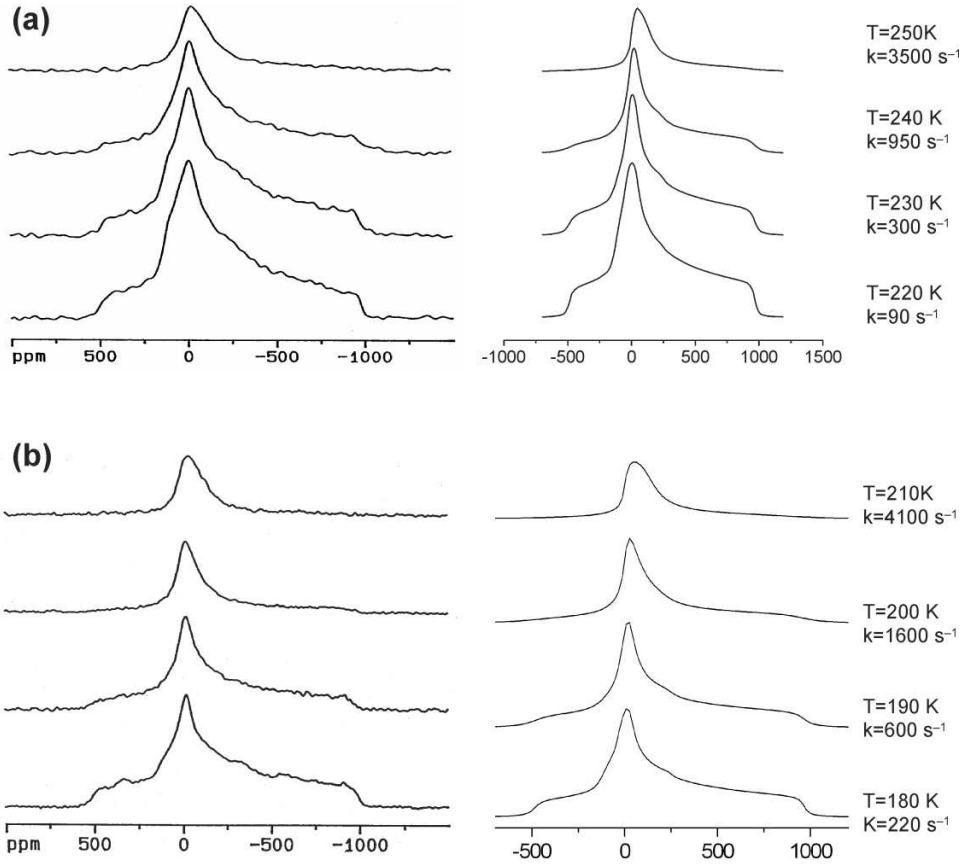

Fig. 7. Experimental plots of ln(*k*) versus 1/*T* for water reorientations in ice-Ih (■) and those in THF gas hydrate (◆) and their corresponding least-square linear fits.

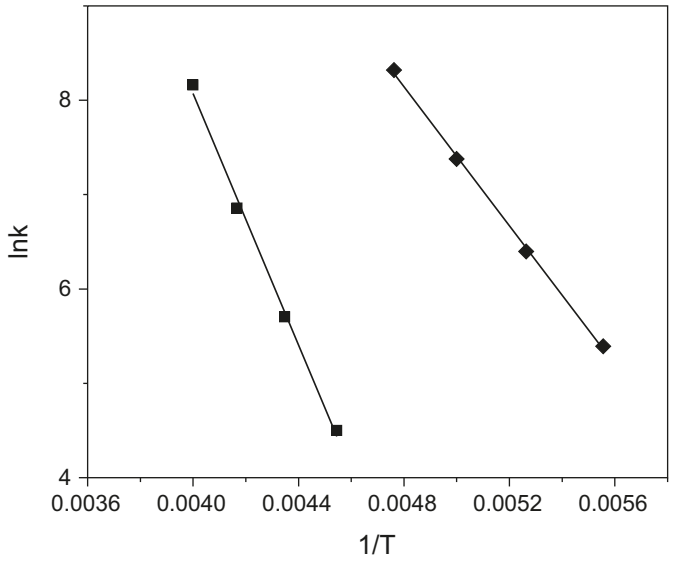

kJ mol^{-1} from ^{2}H NMR.[33,34] This value is smaller than that of ice-Ih, showing that water molecular reorientations in THF gas hydrate are much more facile. As mentioned earlier, it is thought that this is due to injection of Bjerrum L-defects into the hydrate lattice by transient H-bond formation between the O atom of the THF and a water molecule.[10,15,37]

The concurrence of activation energies for both materials with values determined previously affirms the essential correctness of the model in this intermediate regime. If the Arrhenius plots are then extrapolated to 270 K the rates suggested are 2.4×10^4 s^{-1} for ice-Ih and 2.0×10^5 s^{-1} for THF hydrate. The latter value is well towards the fast limit compared with the second-order static linewidth, where the model predicts a residual anisotropic lineshape, but it is also in the range where the first satellite lineshape will be starting to average (recall that ν_Q is $\sim 9.6 \times 10^5$ Hz).

It was mentioned earlier that lower activation energies for water reorientation in hydrates had been ascribed to defect injection by guest molecules containing oxygen.[10,15] Recent molecular dynamics (MD) simulation studies on nanosecond timescales have in fact observed the existence of both transient and persistent guest–host hydrogen bonds for oxygen-containing guests[53–55]. In the simplest cases, this corresponds exactly to the injection of an L-defect as there is indeed a misdirected H-bond, leaving a hydrogen vacancy in the water lattice. Such vacancies will in effect make it easier (lower barrier) for reorientation of an adjacent water molecule to occur. For the more persistent guest–host interactions, a careful study by single crystal X-ray diffraction showed that the misdirected H-bonds to guests could be seen directly (specifically in pinacolone Str.H and t-butylamine Str.II),[56]

indicating that a good fraction of the guests were H-bonded at any particular instant. For stronger guest–host interactions, a water oxygen was also moved out of its usual position in the hydrate cage.[56] However, in the case of THF hydrate the MD simulations showed that these H-bonds are rather short lived (0.28 ps at 200 K), and thus no effects on the structure can be detected.[53] This *injection* of L-defects by the guest appears to be quite a different process from the *propagation* of Bjerrum defects, which governs the water reorientation process as observed by dielectric and NMR relaxation.[10,15] For instance, for THF hydrate the activation energy for L-defect *injection* was found to be ~8.3 kJ/mol from MD simulation,[53] compared with an experimental value of ~30 kJ/mol for defect *propagation* (see refs. 30, 33, 34, 37, and this work). An MD calculation of defect *propagation* will require longer simulation times, as this process barely reaches microsecond timescales at the highest temperatures of study. It may be that the limiting process for defect transport is the ease of D-defect generation.

Conclusion

This study of ^{17}O NMR lineshapes of water in ice and a clathrate hydrate has provided a remarkable picture of the effects of dynamic averaging on lineshapes of a non-integer quadrupolar nucleus over quite a broad range of jump rates. It is also quite consistent with previous studies using other nuclei and other techniques. Apparently, no new details of Bjerrum defect diffusion have come to light, although it is clear that some progress has been made in understanding the role of Bjerrum defect injection and transport in ice and hydrates in general. The observation of an apparently isotropic line that has a second-order shift is quite unusual and could have implications for reporting of shifts in other systems, if it is not recognized that dynamic effects are at play. While rapid reorientation among tetrahedral or octahedral orientations at rates faster than the full first-order linewidth will average the effective electric field gradient to zero, in which case an isotropic line at the true chemical shift is the ultimate spectrum, it is also well recognized that the second-order central transition lineshape will average to an anisotropic shape at rates comparable with its static linewidth. The current work has also partly explored a rate regime between these two situations where the anisotropically averaged second-order lineshape further averages to an isotropic shape which retains a second-order shift. In the absence of variable temperature work where this behaviour becomes apparent, it would be necessary to check whether an isotropic line has a second-order shift by measuring the shift at more than one magnetic field.

Acknowledgement

American Chemical Society Petroleum Research Fund under the award PRF#39645-GB5M is thanked for the partial support of this research.

References

(1) Hobbs, P. V. In *Ice Physics*. Clarendon Press: Oxford., 1974, p. 60–78.
(2) Bragg, W. H. *Proc. Phys. Soc.* **1922** *34*, 98.
(3) Peterson, S. W., Levy, H.A. *Acta Crystallogr.* **1957** *10*, 70 . doi:10.1107/S0365110X5700016X.
(4) Chidambaram, R. *Acta Crystallogr.* **1961** *14* (5), 647. . doi:10.1107/S0365110X61001509.
(5) Pauling, L. *J. Am. Chem. Soc.* **1935** *57* (12), 2680. . doi:10.1021/ja01315a102.
(6) Auty, R. P.; Cole, R. H. *J. Chem. Phys.* **1952** *20* (8), 1309. . doi:10.1063/1.1700726.
(7) Granicher, H.; Jaccard, C.; Scherrer, P.; Steinemann, A. *Discuss. Faraday Soc.* **1958** *23*, 50 . doi:10.1039/df9572300050.
(8) Eisenburg, D.; Kauzman, W. *The Structure and Properties of Water*. Oxford University Press, Oxford, 1969.
(9) Bjerrum, N. *Science* **1952** *115* (2989), 385. . doi:10.1126/science.115.2989.385.
(10) Davidson, D. W. In *Water: A Comprehensive Treatise*, Ed. Franks, F., Plenum Press, New York, 1973, Vol.2, p115–234.
(11) Jeffrey, G. A. In *Comprehensive Supramolecular Chemistry*, Eds. MacNicol, D.D.; Toda, F.; Bishop, R., Pergamon, 1996, Vol.6, 757–788.
(12) Dyadin, Y. A.; Belosludov, V. R. In *Comprehensive Supramolecular Chemistry*, Eds. MacNicol, D.D.; Toda, F.; Bishop, R., Pergamon, 1996, Vol.6, p.789–824.
(13) Sloan, E. D.; Koh, C. A. *Clathrate Hydrates of Natural Gases*. 3rd ed., CRC Press, Boca Raton, 2008.
(14) Cox, J. L. *Natural Gas Hydrates: Properties, Occurrence and Recovery*, Butterworth Press, Woburn, Mass., 1983.
(15) Davidson, D. W.; Ripmeester, J. A. In *Inclusion Compounds*, Eds. Atwood, J.L.; Davies, J.E.D.; MacNicol, D.D., Academic Press, London,1984, Vol.3, p. 69–128.
(16) Davidson, D. W.; Desando, M. A.; Gough, S. R.; Handa, Y. P.; Ratcliffe, C. I.; Ripmeester, J. A.; Tse, J. S. *Nature* **1987** *328* (6129), 418. . doi:10.1038/328418a0.
(17) Ripmeester, J. A.; Davidson, D. W. *Molecular Crystals and Liquid Crystals* **1977** *43* (3), 189. . doi:10.1080/00268947708084666.
(18) Ripmeester, J. A.; Ratcliffe, C. I. *J. Phys. Chem.* **1990** *94* (25), 8773. . doi:10.1021/j100388a006.
(19) Mak, T. C. W.; McMullan, R. K. *J. Chem. Phys.* **1965** *42* (8), 2732. . doi:10.1063/1.1703229.
(20) McMullan, R. K.; Kvick, A. *Acta Crystallogr.* **1990** *B46*, 390.
(21) Ratcliffe, C. I.; In, N. M. R. *Crystallography*, Eds. Harris, R. K.; Wasylishen, R.E.; Duer, M.J., Wiley, Chichester UK, 2009, p. 355–373.
(22) Vega, A. J.; Luz, Z. *J. Phys. Chem.* **1987** *86* (4), 1803. . doi:10.1063/1.452181.
(23) Wittebort, R. J.; Olejniczak, E. T.; Griffin, R. G. *J. Chem. Phys.* **1987** *86* (10), 5411. . doi:10.1063/1.452565.
(24) Barnaal, D. E.; Lowe, I. J. *J. Chem. Phys.* **1968** *48* (10), 4614. . doi:10.1063/1.1668036.
(25) Siegle, G.; Weithase, M. *Z. Phys.* **1969** *219* (4), 364. . doi:10.1007/BF01395533.
(26) Weithase, M.; Noack, F.; von Schutz, J. *Z. Phys.* **1971** *246*, 91 . doi:10.1007/BF01402654.
(27) Valic, M. I.; Gornostansky, S.; Pintar, M. M. *Chem. Phys. Lett.* **1971** *9* (4), 362. . doi:10.1016/0009-2614(71)80243-9.
(28) Wittebort, R. J.; Usha, M. G.; Ruben, D. J.; Wemmer, D. E.; Pines, A. *J. Am. Chem. Soc.* **1988** *110* (17), 5668. . doi:10.1021/ja00225a013.
(29) Blinc, R.; Lahajnar, G.; Zupancic, I.; Granicher, H. *Chem. Phys. Lett.* **1969** *4*, 363.
(30) Garg, S. K.; Davidson, D. W.; Ripmeester, J. A. *J. Magn. Reson.* **1974** *15*, 295.
(31) Schmidt, V. H. In *Physics and Chemistry of Ice*, Ed. Whalley,

E.; Jones, S.J.; Gold, L.W., Roy. Soc. Canada, Ottawa, 1973, 212–217.
(32) Davidson, D. W.; Garg, S. K.; Ripmeester, J. A. *J. Magn. Reson.* **1978** *31*, 399.
(33) Bach-Verges, M.; Kitchin, S. J.; Harris, K. D. M.; Zugic, M.; Koh, C. A. *J. Phys. Chem. B* **2001** *105* (14), 2699. . doi:10.1021/jp002529o.
(34) Kirschgen, T. M.; Zeidler, M. D.; Geil, B.; Fujara, F. *Phys. Chem. Chem. Phys.* **2003** *5* (23), 5243. . doi:10.1039/b212471h.
(35) Kirschgen, T. M.; Zeidler, M. D.; Geil, B.; Fujara, F. *Phys. Chem. Chem. Phys.* **2003** *5* (23), 5247. . doi:10.1039/b212472f.
(36) Bach-Verges, M.; Kitchin, S. J.; Harris, K. D. M.; Zugic, M.; Koh, C. A. *Phys. Chem. Chem. Phys.* **2004** *6*, 871 . doi:10.1039/b307944a.
(37) Gough, S. R.; Hawkins, R. E.; Morris, B.; Davidson, D. W. *J. Phys. Chem.* **1973** *77* (25), 2969. . doi:10.1021/j100643a009.
(38) Witschas, M.; Eckart, H.; Freiheit, H.; Putnis, A.; Korus, G.; Jansen, M.et al. *J. Phys. Chem. A* **2001** *105* (28), 6808. . doi:10.1021/jp003635t.
(39) Kristensen, J. H.; Farnan, I. *J. Chem. Phys.* **2001** *114* (21), 9608. . doi:10.1063/1.1368660.
(40) Schurko, R. W.; Wi, S.; Frydman, L. *J. Phys. Chem. A* **2002** *106* (1), 51. . doi:10.1021/jp0130214.
(41) Witschas, M.; Eckert, H. *J. Phys. Chem. A* **1999** *103* (50), 10764. . doi:10.1021/jp992763i.
(42) Muller, K. *Phys. Chem. Chem. Phys.* **2002** *4*, 5515 . doi:10.1039/b206852d.
(43) Ashbrook, S. E.; Antonijevic, S.; Berry, A. J.; Wimperis, S. *Chem. Phys. Lett.* **2002** *364* (5-6), 634. . doi:10.1016/S0009-2614(02)01412-4.
(44) Ba, Y.; Ratcliffe, C. I.; Ripmeester, J. A. *Chem. Phys. Lett.* **1999** *299* (2), 201. .[This is a re-interpretation of single crystal data by Waldstein, P.; Rabideau, S.W., J.Chem.Phys., 1967, 47, 5338-5342]. doi:10.1016/S0009-2614(98)01275-5.
(45) Kunwar, A. C.; Turner, G. L.; Oldfield, E. *J. Magn. Reson.* **1986** *69*, 124.
(46) Spiess, H. W.; Garrett, B. B.; Sheline, R. K.; Rabideau, S. W. *J. Chem. Phys.* **1969** *51* (3), 1201. . doi:10.1063/1.1672122.
(47) Edmonds, D. T.; Zussman, A. *Phys. Lett.* **1972** *41A*, 167.
(48) Edmonds, D. T.; Goren, S. D.; Mackay, A. L.; White, A. A. L.; Sherman, W. F. *J. Magn. Reson.* **1976** *23*, 504.
(49) Zhang, Q. W.; Zhang, H. M.; Usha, M. G.; Wittebort, R. J. *Sol. Stat.NMR* **1996** *7* (3), 147. . doi:10.1016/S0926-2040(96)01258-1.
(50) Schporer, M.; Achlama, A. M. *J. Chem. Phys.* **1976** *65*, 3657 . doi:10.1063/1.433553.
(51) Pennanen, T. S.; Vaara, J.; Lantto, P.; Sillanpaa, A. J.; Laasonen, K.; Jokisaari, J. *J. Am. Chem. Soc.* **2004** *126* (35), 11093. . doi:10.1021/ja048049i.
(52) Man, P. P. In *Encylopedia of NMR*, Eds. Grant, D.M.; Harris, R.K., John Wiley, New York, 1996, p. 3838–47.
(53) Alavi, S.; Susilo, R.; Ripmeester, J. A. *J. Chem. Phys.* **2009** *130* (17), 174501. . doi:10.1063/1.3124187.
(54) Susilo, R.; Alavi, S.; Moudrakovski, I. L.; Englezos, P.; Ripmeester, J. A. *ChemPhysChem* **2009** *10* (5), 824. . doi:10.1002/cphc.200900024.
(55) Alavi, S.; Takeya, S.; Ohmura, R.; Woo, T. K.; Ripmeester, J. A. *J. Chem. Phys.* **2010** *133* (7), 074505. . doi:10.1063/1.3469776.
(56) Alavi, S.; Udachin, K.; Ripmeester, J. A. *Chemistry* **2010** *16*, 1017.